A uniform source-and-sink scheme for calculating thermal conductivity by nonequilibrium molecular dynamics

Bing-Yang Cao (曹炳阳)[a] and Yuan-Wei Li (李元伟)
Department of Engineering Mechanics, Key Laboratory for Thermal Science and Power Engineering of Ministry of Education, Tsinghua University, Beijing 100084, People's Republic of China

(Received 22 May 2010; accepted 23 June 2010; published online 14 July 2010)

A uniform source-and-sink (USS) scheme, which combines features of the reverse [F. Müller-Plathe, J. Chem. Phys. **106**, 6082 (1997)] and improved relaxation [B. Y. Cao, J. Chem. Phys. **129**, 074106 (2008)] methods, is developed to calculate the thermal conductivity by nonequilibrium molecular dynamics (NEMD). The uniform internal heat source and sink are realized by exchanging the velocity vectors of individual atoms in the right half and left half systems, and produce a periodically quadratic temperature profile throughout the system. The thermal conductivity can be easily extracted from the mean temperatures of the right and left half systems rather than by fitting the temperature profiles. In particular, this scheme greatly increases the relaxation of the exited localized phonon modes which often worsen the calculation accuracy and efficiency in most other NEMD methods. The calculation of the thermal conductivities of solid argon shows that the simple USS scheme gives accurate results with fast convergence. © *2010 American Institute of Physics*. [doi:10.1063/1.3463699]

Since "the thermal conductivity has proven to be one of the most difficult transport coefficients to calculate,"[1] great efforts have been made over the years to develop molecular dynamics (MD) schemes to simulate the thermal conductivity of matters (see Refs. 2–4 and references therein). Nonequilibrium molecular dynamics (NEMD) methods have been demonstrated to converge faster than equilibrium molecular dynamics (EMD) methods. However, heat source and sink slabs have to be used in the NEMD schemes to inject and remove energy to set up a temperature difference or heat current. The heat injection and removal may excite localized phonon modes in edge regions and result in significant temperature jumps,[5–11] which are very harmful to the MD calculation accuracy and simulation efficiency. Recently, Jiang *et al.*[12] reported that the localized edge modes could be conquered by shifting the source and sink slabs away from the edge regions of the simulation system as the excited vibrations relaxed very quickly.

The purpose of the present paper is to develop a new NEMD method which can eliminate the temperature jump effects and facilitate the calculation based on the following three points. First, using internal heat source and sink will be helpful for enhancing the relaxation of the excited vibrations.[12] Heating and cooling individual atoms give the highest relaxation rate for the localized vibrations excited by the energy injection and removal in MD calculations.[4,13] Second, the relaxation-improved scheme in Ref. 4, which used uniform heat source and sink based on heating and cooling individual molecules, is thus preferable except that the Maxwell-like energy perturbation seems sort of complicated and unnecessary. In addition, this method has advantages at the thermal conductivity extraction and calculation convergence. Third, the reverse NEMD method[14,15] really has many good features, such as homogeneity, convergence, periodic boundary conditions (PBCs), conservation of energy and momentum, and Hamiltonian. It has been further developed and is more and more popular in calculating the thermal conductivity.[16–21] Inspired by the above mentioned points, we can infer that a better option is to incorporate these good features of different NEMD schemes.

We herewith develop a uniform source-and-sink (USS) scheme to combine features of the reverse,[14] improved relaxation[4] and eliminated edge mode[12] methods to calculate the thermal conductivity by NEMD, as shown in Fig. 1. Periodic boundary conditions are applied along the x, y, and z directions. The velocity vector exchanges are similar to the strategy put forward by Ref. 14 except that the heat source and sink slabs are frequently changed so that the uniform internal heat source and sink can be obtained. The simulation box is divided into N slabs in the x direction. The hottest atom in slab_i in the left half system exchanges velocity vectors with the coldest atom in slab_j in the right half system so as to generate an internal heat sink in the left half system and an internal heat source in the right half system. This velocity exchanges are equivalent to injecting energy into and removing energy from individual atoms. It should be noted that the velocity vector exchange is much simpler than the Maxwell distributed energy perturbation in the previous literature.[4] Every simulation step for exchanging velocity vectors, the slab_i and slab_j are always selected to have minimum energy generation and removal rates among all slabs, respectively, in the left and right half systems, which makes sure that the heat source and sink will go uniform. Therefore, the heat source/sink density (energy generation per time per volume,

[a]Author to whom correspondence should be addressed. Tel./FAX: 86-10-6278-1610. Electronic mail: caoby@tsinghua.edu.cn.

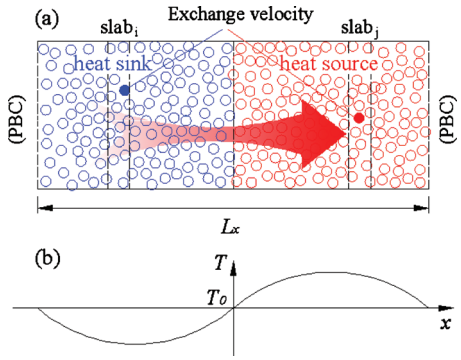

FIG. 1. Schematic diagrams of (a) the NEMD simulation system applying the USS scheme and (b) the temperature profile.

with a negative value meaning the energy removal rate) can be written as

$$q_v = \frac{\Sigma_{\text{transfers}} m(v_h^2 - v_c^2)}{tL_xL_yL_z}, \tag{1}$$

in which L_x, L_y, L_z are the box lengths in x, y, z directions, respectively, t is the simulation time, m is the mass of an atom, and v_h and v_c are the velocities of the hottest and coldest atoms, respectively. Every W time steps, we perform a velocity vector exchange between two atoms lying in the left and right half systems separately. Thus, the heat source and sink density only depend on the exchange interval W in the simulations. For steady state and one dimensional heat conduction, the uniform heat source and sink with PBC lead to an almost sinusoidal temperature profile, as shown in Fig. 1(b),

$$T = \begin{cases} \dfrac{q_v}{2\lambda}\left(x + \dfrac{L_x}{4}\right)^2 - \dfrac{q_v L_x^2}{32\lambda} + T_0, & \left(-\dfrac{L_x}{2} \le x < 0\right) \\ \dfrac{-q_v}{2\lambda}\left(x - \dfrac{L_x}{4}\right)^2 + \dfrac{q_v L_x^2}{32\lambda} + T_0, & \left(0 \le x \le \dfrac{L_x}{2}\right). \end{cases} \tag{2}$$

Here T_0 is the mean temperature of the entire system, and λ is the thermal conductivity. The imposed energy transfer is balanced by heat conduction within the system. The mean temperatures of the left and right halves of the system depend directly on the thermal conductivity. Then, the thermal conductivity can be extracted from the left and right mean system temperatures,[4]

$$\lambda = \frac{q_v L_x^2}{48\Delta T}. \tag{3}$$

The features of the USS scheme are worthy of mentioning here according to the above simulation procedure. First, the energy injection and removal in the present scheme are realized by velocity vector exchanges, which are originally introduced by the reverse NEMD method.[14] The USS scheme surely has all good features of the reverse NEMD method, such as homogeneity, PBC, energy conservation, momentum conservation, and Hamiltonian. Second, by imposing uniform heat source and sink, the thermal conductivity can be calculated directly from the mean temperatures of the right and left half systems rather than by fitting the temperature gradient. This facilitates the statistics of the thermal conductivity as a feature of the improved relaxation method.[4] Third, the velocity exchanges are imposed in two small slabs in the reverse NEMD method, and are now on individual molecules throughout the entire system in the USS scheme. This maximizes the relaxation rate of the energy injection and removal perturbations, and maximally enhances the relaxation of the excited localized phonon modes.[12,13]

We calculate the thermal conductivity of solid argon to verify the present USS scheme. It should be mentioned that the USS scheme can also give good results of liquid argon, as demonstrated in Ref. 4. Argon is simulated because its atomic dynamics can be described with very good accuracy by a simple Lennard-Jones (LJ) pair potential and many benchmark results for the thermal conductivity are available in previous literature. The particle interactions are described by the LJ potential in the form

$$\phi(r) = 4\varepsilon\left[\left(\frac{\sigma}{r}\right)^{12} - \left(\frac{\sigma}{r}\right)^{6}\right], \tag{4}$$

where r is the intermolecular distance, ε is the energy parameter, and σ is the molecular diameter. The parameters used in this paper are $\varepsilon = 1.67 \times 10^{-21}$ J and $\sigma = 3.41 \times 10^{-10}$ m.[22] For convenience, rescaled units are used for most physical parameters as indicated by the superscript $*$ (see Table I in Ref. 4). The equations of motion for the molecules are integrated by using a leapfrog Verlet algorithm[23] with a time step of $dt = 0.005\tau$. The time-consuming calculations of the interparticle interactions are reduced by using a potential cutoff of $r_{\text{cut}} = 2.5\sigma$ and a cell-linked list method.[23]

The solid argon is simulated as a face-centered cubic crystal with a lattice constant $a = 1.5591\sigma$, which corresponds to a numerical density $n^* = 1.0554$ of solid argon at a pressure of 5 atm.[24] The lengths of the simulation box in the y and z directions are set to $L_y = L_y = 7.8\sigma$, with L_x adjusted to observe the size effects. The simulations include 1000–12 000 molecules with L_x ranging from 15.6σ to 93.6σ. Each run allows 1500τ (300 000 time steps) for the system to reach a steady state heat conduction, then the left and right mean temperatures, the local temperatures in the slabs, and the heat source and sink densities are averaged over another $1500-3000\tau$ (300 000–600 000 time steps). The local temperatures are calculated to show the temperature distribution across the system for examining the uniform heat source and sink based scheme, although they are not necessary for the thermal conductivity calculation.

Typical temperature profiles with $L_x = 31.2\sigma$ are shown in Fig. 2(a) for three different velocity exchange intervals. The uniform heat source and sink scheme along with the periodic boundary conditions leads to a quadratic temperature profile. As a result, the temperature profiles in both the left and right halves are quadratic and can be fit by quadratic functions, which agrees with Eq. (2). It confirms that the present USS scheme produces ideally uniform internal source and sink, as shown in Fig. 2(b). The consecutive temperature curves are indicative of the complete relaxation of the localized phonon modes by using the internal heat source

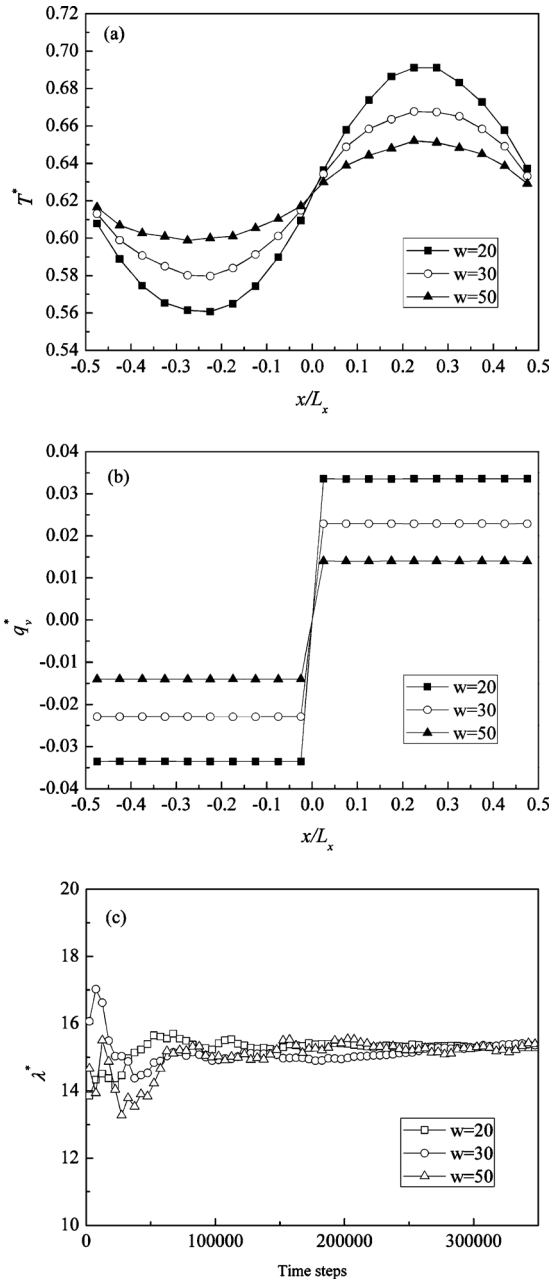

FIG. 2. (a) Temperature profiles, (b) heat source and sink densities, and (c) time averaged thermal conductivities for various velocity exchange intervals (L_x=31.2σ).

and sink. The left and right mean temperatures depend on the heat source and sink density, i.e., the velocity exchange interval W. A stronger heat source and sink density, or a smaller W, as indicated in Fig. 2(b), always results in larger temperature differences throughout the system. The left and right mean temperatures can then be used to calculate the thermal conductivity of the solid according to Eq. (3).

The time averaged thermal conductivities are shown in Fig. 2(c) for W=20, 30, and 50. The thermal conductivity initially has large fluctuation but then quickly converges. The results show that the simulations often need about 1500τ (3×10^5 time steps) to obtain a converged result for the thermal conductivity, which is much less than the primary estimate of 5000τ for the reverse NEMD scheme.[19] These results imply that the left and right mean temperatures converge much faster than data collected in slabs containing fewer molecules.

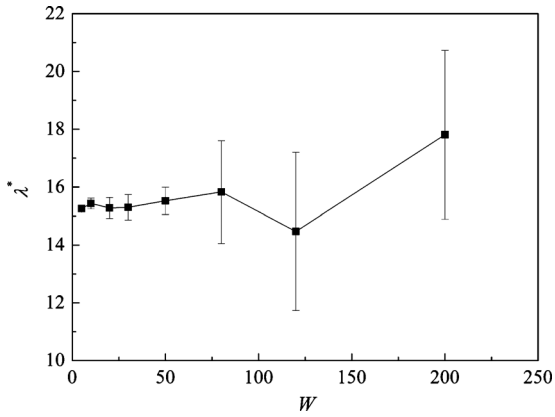

FIG. 3. Dependence of the calculated thermal conductivity on the velocity exchange interval (L_x=31.2σ).

The dependence of the calculated thermal conductivity on the velocity exchange interval is shown in Fig. 3. The uncertainty of the thermal conductivity is obtained by the statistical error of the thermal conductivity fluctuation along with time. With W=2, the relative uncertainty of the calculated thermal conductivity is only about ±0.2%. The uncertainty increases to ±16.4% when W=25. Then mean thermal conductivity is estimated to be λ^*=15.56 by the nine data. The total uncertainty is within ±5.9%. The thermal conductivity uncertainty decreases as the thermal perturbation strength increases with the same averaging time. The simulations also indicate that for the weaker perturbation, i.e., the larger exchange interval, a longer time should be required to establish the steady state heat conduction and to average the statistical samples.

In order to verify the applicability of the linear response theory, we plot the relation between the heat flux and the temperature gradient in Fig. 4. The data are collected from the simulation case with the largest perturbation, i.e. W=5. In this simulation, the maximal temperature difference is about $0.4\varepsilon/k_B$, and the temperature gradient ranges from

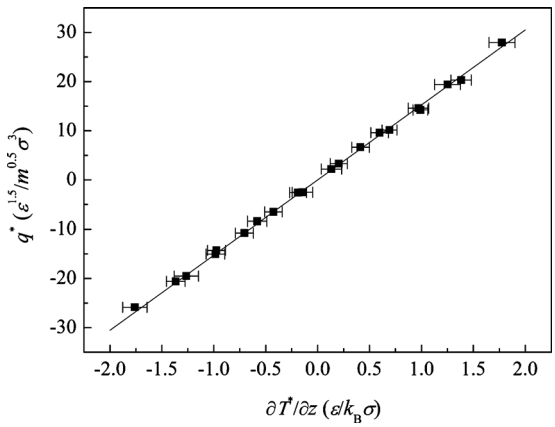

FIG. 4. Relation between the heat flux and the temperature gradient. Data are collected from a simulation case with L_x=31.2σ, W=5, and q_v^*=0.11. Error bars denote the standard error of fitting the temperature profile by a least-squares method.

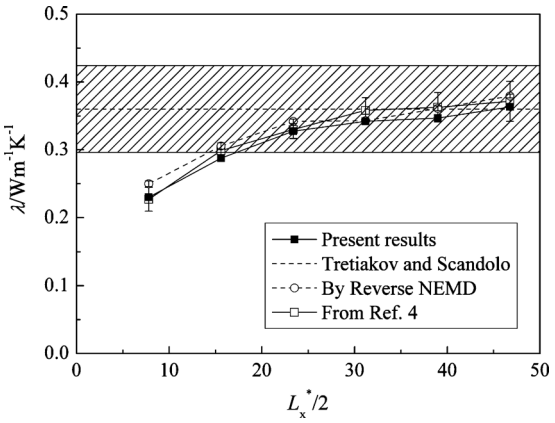

FIG. 5. Dependence of the thermal conductivity on the system size. The cross-hatched block represents the uncertainty of the EMD results by Tretiakov and Scandolo (Ref. 25).

$-2\varepsilon/k_B\sigma$ to $2\varepsilon/k_B\sigma$. Figure 4 clearly shows that the linear response holds for all and even our largest perturbation ($W=5$).

The calculated solid argon thermal conductivities for various system sizes are presented in Fig. 5. Here, the system size is defined as the half width of the system in the x direction (i.e., $L_x/2$). The reference value was obtained using an EMD method and has been demonstrated to have very small size effects.[25] First, the present USS scheme can give very close results to those by the reverse and improved relaxation NEMD methods. This confirms that the USS scheme gives accurate results. Second, the thermal conductivity increases as the system size increases because of the size effects. The USS, reverse, and relaxation-improved schemes have same tendencies. It indicates that the USS scheme may also be applied to study the size effects of the thermal conductivity.[26] Since the USS scheme is based on the Fourier's heat conduction law which can only characterize diffusive heat conduction, the scheme is inapplicable to investigate the thermal properties of low-dimensional materials in which the ballistic transport dominates. However, the present USS scheme may be useful for studying the heat transport mechanisms in low-dimensional materials with internal heat sources as practically applied to measure the thermal properties of carbon nanotubes[27,28] and metallic nanofilms.[29,30] Third, velocity exchange intervals from 10 to 100 give better results keeping in mind that smaller intervals lead to larger temperature difference in the system and larger intervals lead to larger uncertainty and computation burden.

In summary, a uniform source-and-sink scheme is developed to calculate the thermal conductivity by nonequilibrium molecular dynamics. We are convinced that the scheme combines the features of the original reverse and improved relaxation methods with the inspiration of eliminating localized phonon modes method from Ref. 12. The calculation of the thermal conductivity of solid argon shows that the simple USS scheme gives accurate results with fast convergence. The features of the USS scheme are worthy of mentioning. (i) The heat source and sink are produced by exchanging the velocity vectors of atoms in the right half and left half systems. The velocity vector exchange is much simpler than the Maxwell distributed energy perturbation in Ref. 4. To perform the USS simulation is as simple as the original reverse NEMD. (ii) The heat source and sink are uniformly distributed in the right and left halves of the system, which leads to a quadratic temperature distribution. The thermal conductivity can be easily calculated from the left and right mean temperatures by using the Fourier's heat conduction law. The statistics of the thermal conductivity has small uncertainty and fast convergence. (iii) By using internal heat source and sink, the relaxation of the excited phonon modes can be maximally enhanced. Therefore, there is no temperature jump throughout the simulation system. It further benefits the calculation accuracy and efficiency compared with most other NEMD methods. (iv) The USS scheme gives accurate results compared with the original reverse NEMD method. We then hope that its application can also be extended to liquids, polymers, soft matters, nanocomposites, and even the thermal transport in low-dimensional materials with internal heat sources or sinks.

We are very grateful to the reviewers for their in-depth suggestions toward improving our manuscript. This work is financially supported by the National Natural Science Foundation of China (Grant Nos. 50976052, 50606018, and 50730006) and the Tsinghua National Laboratory for Information Science and Technology (TNList) Cross-discipline Foundation.

[1] D. J. Evans and G. P. Morris, *Statistical Mechanics of Nonequilibrium Liquids* (Academic, London, 1990).
[2] P. Ungerer, C. Neito-Draghi, B. Rousseau, G. Ahunbay, and V. Lachet, J. Mol. Liq. **134**, 71 (2007).
[3] P. Heino, J. Comput. Theor. Nanosci. **4**, 896 (2007).
[4] B. Y. Cao, J. Chem. Phys. **129**, 074106 (2008).
[5] P. K. Schelling, S. R. Phillpot, and P. Keblinski, Phys. Rev. B **65**, 144306 (2002).
[6] P. Chantrenne and J. L. Barrat, ASME Trans. J. Heat Transfer **126**, 577 (2004).
[7] G. Zhang and B. Li, J. Chem. Phys. **123**, 114714 (2005).
[8] P. Heino, Phys. Rev. B **71**, 144302 (2005).
[9] J. Shiomi and S. Maruyama, Jpn. J. Appl. Phys., Part 1 **47**, 2005 (2008).
[10] S. C. Wang, X. G. Liang, X. H. Xu, and T. Ohara, J. Appl. Phys. **105**, 014316 (2009).
[11] M. Alaghemandi, F. Leroy, E. Algaer, M. C. Böhm, and F. Müller-Plathe, Nanotechnology **21**, 075704 (2010).
[12] J. W. Jiang, J. Chen, J. S. Wang, and B. W. Li, Phys. Rev. B **80**, 052301 (2009).
[13] B. L. Holian, J. Chem. Phys. **117**, 1173 (2002).
[14] F. Müller-Plathe, J. Chem. Phys. **106**, 6082 (1997).
[15] F. Terao and F. Müller-Plathe, J. Chem. Phys. **123**, 217101 (2005).
[16] D. Bedrov and G. D. Smith, J. Chem. Phys. **113**, 8080 (2000).
[17] C. Nieto-Draghi and J. B. Avalos, Mol. Phys. **101**, 2303 (2003).
[18] M. Zhang, E. Lussetti, L. E. S. de Souza, and F. Müller-Plathe, J. Phys. Chem. B **109**, 15060 (2005).
[19] R. D. Mountain, J. Chem. Phys. **124**, 104109 (2006).
[20] T. Terao, E. Lussetti, and F. Müller-Plathe, Phys. Rev. E **75**, 057701 (2007).
[21] E. Rossinsky and F. Müller-Plathe, J. Chem. Phys. **130**, 134905 (2009).
[22] G. C. Maitland, M. Rigby, E. B. Smith, and W. A. Wakeham, *Intermolecular Forces: Their Origin and Determination* (Clarendon, Oxford, 1981).
[23] M. P. Allen and D. J. Tildesley, *Computer Simulation of Liquids* (Oxford University, New York, 1989).
[24] O. G. Peterson, D. N. Batchelder, and R. O. Simmons, Phys. Rev. **150**, 703 (1966).
[25] K. V. Tretiakov and S. Scandolo, J. Chem. Phys. **120**, 3765 (2004).
[26] X. G. Liang, Chin. Sci. Bull. **52**, 2457 (2007).

[27] E. Pop, D. Mann, Q. Wang, K. Goodson, and H. J. Dai, Phys. Rev. Lett. **95**, 155505 (2005).
[28] E. Pop, D. Mann, Q. Wang, K. Goodson, and H. J. Dai, Nano Lett. **6**, 96 (2006).
[29] Q. G. Zhang, X. Zhang, B. Y. Cao, M. Fujii, K. Takahashi, and T. Ikuta, Appl. Phys. Lett. **89**, 114102 (2006).
[30] Q. G. Zhang, B. Y. Cao, X. Zhang, M. Fujii, and K. Takahashi, Phys. Rev. B **74**, 134109 (2006).